Silicon-based mesoporous photonic crystals: towards single cell optical biosensors

Kilian, Kristopher, Magenau, Astrid, Böcking, Till, Gaus, Katharina, Gal, Michael, et al.

Kristopher A. Kilian, Astrid Magenau, Till Böcking, Katharina Gaus, Michael Gal, J. Justin Gooding, "Silicon-based mesoporous photonic crystals: towards single cell optical biosensors," Proc. SPIE 7397, Biosensing II, 739703 (21 August 2009); doi: 10.1117/12.826133

SPIE.

Event: SPIE NanoScience + Engineering, 2009, San Diego, California, United States

Silicon-based mesoporous photonic crystals: towards single cell optical biosensors

Kristopher A. Kilian*[a], Astrid Magenau[c], Till Böcking[a,b], Katharina Gaus[c], Michael Gal[b], and J. Justin Gooding*[a]

[a]Dept. of Chemistry, [b]Dept. of Physics, [c]Centre for Vascular Research, University of New South Wales, Sydney, NSW, Australia 2052

ABSTRACT

Mesoporous silicon (PSi) photonic crystals have attracted interest as biosensing transducers owing to their high quality optics and sensitivity in optical characteristics to changes in refractive index. We describe progress our group has made derivatizing PSi towards devices for biology and medicine. PSi rugate filters display a high reflectivity resonant line in the reflectance spectrum. As an example for biosensing, immobilization of peptides and biopolymers within the PSi is demonstrated for detecting protease enzymes. Secretion of matrix metalloproteases from live cells was detected as a blue shift in the photonic resonance within hours, demonstrating the promise of this biosensor.

Keywords: Porous silicon, photonic crystal, biosensor, protease, cell culture

1. INTRODUCTION

Nanostructured porous silicon (PSi) is formed by anodic etching of Si(100) in an ethanolic hydrofluoric acid solution. Computer control over the current during the electrochemical etch allows spatial control over the nanoarchitecture and thin film optical properties. Multilayered PSi materials constitute one-dimensional photonic crystals where the type of crystal and photonic band-gap can be easily modified by adjustment of the etching parameters. In this way, Fabry-Perot thin films, bragg reflectors, resonant microcavities and rugate filters have been demonstrated.[1]

PSi photonic crystals have attracted interest as materials for biology and transducers of biological signals over the past several decades.[1-5] Due to the biocompatibility of PSi and the sensitivity to changes in refractive index within the photonic material, numerous groups have investigated the utility of PSi as a substrate for cell biology studies.[6-14] Despite progress in this area, only a few reports capitalize on the photonic response of PSi to refractive index changes induced by the adherent cell.[6, 12, 14]

In this paper, we present an update on our efforts to incorporate PSi thin film photonic materials into standard cell culture. Rugate filters fabricated by a sinusoidal variation in current during anodization are either left on the crystalline silicon support or removed by a short high density current pulse. These films are first stabilized by hydrosilylation of alkenes then further modified for biomolecule immobilization to define a specific biorecognition interface (Figure 1a). Using this robust chemical and biological modification strategy, we show how PSi rugate filters modified with an extra-cellular matrix biopolymer (gelatin) allow detection of secreted protease enzymes from live J447 murine macrophage cells.

2. MATERIALS AND METHODS

2.1 Materials

All materials, chemicals and reagents were purchased from Sigma-Aldrich unless otherwise specified. MMP-2 (crude Collagenase IV from Clostridium histolyticum) was purchased from Sigma-Aldrich. C-terminus aminated peptide GRGDS was purchased from GenScript Corporation (NJ, USA)

Biosensing II, edited by Manijeh Razeghi, Hooman Mohseni, Proc. of SPIE Vol. 7397, 739703 · © 2009 SPIE · CCC code: 0277-786X/09/$18 · doi: 10.1117/12.826133

2.2 Porous Silicon Rugate Filters

p^+-type Si(100), resistivity 0.005 Ω cm, was cleaned first in acetone followed by ethanol with sonication for 5 minutes each. The wafer was dried and placed in an electrochemical cell as described previously.[15] Briefly, the wafer is back-contacted with a polished steel electrode and the etching cell filled with 25% HF in ethanol (equal parts 50% HF in water and absolute ethanol). A circular platinum electrode is immersed in the ethanolic HF solution above the wafer. A current density alternating between 250 mA/cm^2 and 450 mA/cm^2 was applied to the cell sinusoidally with index matching, apodization and current breaks (to retain electrolyte concentration at dissolution front). After etching, the wafer was rinsed with ethanol and pentane, dried with argon and stored until use.

2.3 Hydrosilylation, Coupling, Activation and Gelatin Immobilisation.

10-succinimidyl undecenoate in mesitylene (0.2 M) was added to a flame dried Schlenk flask under argon degassed by five freeze-pump-thaw cycles (liquid N_2, high vacuum, T_{room}) and held at room temperature under an argon atmosphere. After placing the PSi sample into the degassed alkene solution, the reaction was brought to 90 - 120˚ C and reacted for approximately 24 hours. For different modification of the PSi surface, triethylsilyl chloride was added to the solution (20 mM) and refluxed at 170˚ C for 15 minutes prior to sample loading (see reference[12]). After hydrosilylation at 150˚ C for 12 hours, aqueous solution of peptide GRGDS was reacted with the surface of the rugate filters for 30 minutes at room temperature followed by rinsing with water and ethanol. After rinsing and drying under a stream of nitrogen, coupling of 1-amino hexaethyleneglycol (20 mM in acetonitrile) occurred in 4-8 hours. Activation of distal hydroxyl groups was performed by immersing PSi samples in a 0.1 M solution of disuccinimidyl carbonate (DSC) in dry acetonitrile (under molecular sieves) containing 0.1 M 4-dimethylaminopyridine (DMAP) for 12 - 24 hours, followed by rinsing with ethyl acetate and CH_2Cl_2 and blown dry under a stream of argon. Gelatin (from porcine skin, 60g low bloom, Fluka BioChemika) immobilization occurred by incubating the activated sample with 300 mg/mL in MilliQ water for 30 minutes at 37˚ C, brought to room temperature and casted at 4˚ C for 30 minutes.

2.4 Optical Measurements of Proteolysis

Gelatin modified samples were placed in a quartz cuvette (5 mm x 1 cm x 5 cm), covered with parafilm and incubated with ~100 µL of enzyme in phosphate buffered saline at 37˚ C in a circulating water bath. After cell culture and fixation, surfaces were transferred to cuvettes under PBS for reflectivity measurements. At various time points, the cuvettes were removed from the bath and the reflectivity measurements gathered.

2.5 Cell Culture, Stimulation and Processing

J774 murine macrophages (ATCC) were starved overnight in RPMI (Roswell Park Memorial Institute) medium (0.3 mg/mL L-glutamine, 1µg/mL folic acid, 0.02 mg/mL sodium bicarbonate) with 1 mg/mL bovine serum albumin (BSA). CellTracker Orange (CMRA, Invitrogen) was prepared to 10 mM in DMSO, 1 µL added to 1 mL of cells and incubated at 37˚ C for 30 minutes. The CMRA media was replaced with fresh RPMI containing 10 % fetal calf serum (FCS) and incubated at 37˚ C for 30 minutes. The cells were removed by scraping, counted and replated over the porous silicon photonic crystals in a 48-well plate at 500 µL ($5x10^5$ cells). The cells were allowed to adhere for 3 hours at 37˚ C with 5 % CO_2 (verified under microscope) and lipopolysaccharide (LPS, from E. Coli) was added to select surfaces at 100 ng/mL. Samples were transferred from media to PBS, imaged by microscopy and the reflectivity spectrum of the PSi measured prior to fixation. Cells were fixed with 4 % paraformaldehyde in phosphate buffered saline ((v/v) PBS). The cell media was spun down to remove detached cells and stored at -20˚C for further characterisation.

2.6 Spectroscopy and Microscopy

Scanning electron micrographs were taken using a Hitachi S900 SEM with a cold field emission source (12 kV). PSi samples were cleaved in the centre of the film and mounted on a brass sample base such that the sample face of interest would be facing the electron beam. Electron conductivity was increased on the semi-conducting sample by using conducting silver paste at the sample edges. For epifluorescence measurements after cell culture, the PSi samples were removed from media and inverted onto phosphate buffered saline covered glass coverslips. Adherent CMRA labelled macrophages were imaged wet using a Nikon Eclipse TE 2000-5 microscope with a 10x objective lens and green filter. Images were collected with Image Pro Plus 5.1 and analysed using ImageJ.

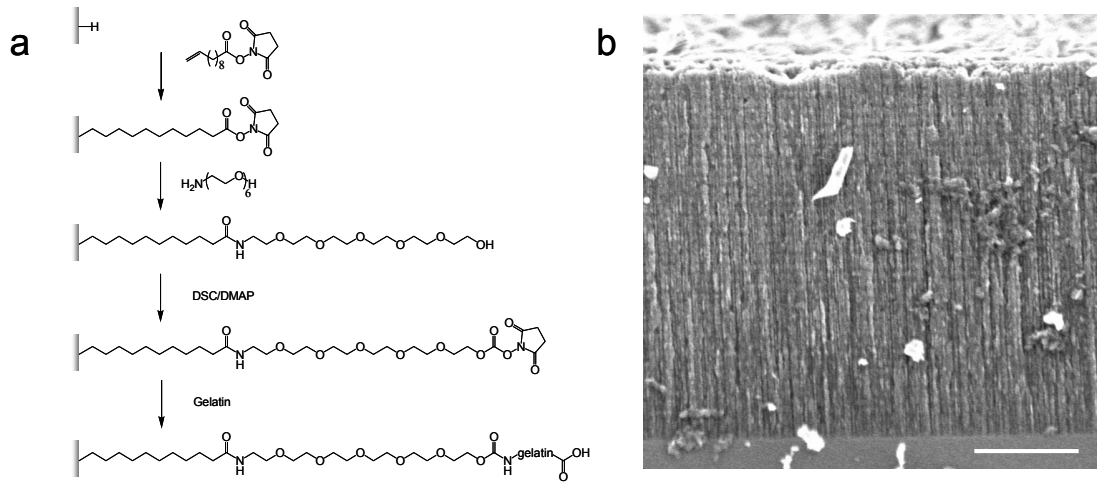

Figure 1. a) Chemical scheme for modification of PSi rugate filters. Hydrosilylation of 10-succinimidyl undecenoate, coupling of amino-EG_6, activation with disuccinimidyl carbonate and gelatin immobilization. b) Side-view scanning electron micrograph of gelatin modified rugate filter thin film. Scale bar = 2 μm

3. RESULTS AND DISCUSSION

Figure 1 shows the chemical scheme for modifying rugate filters for cell culture and a scanning electron microscopy after gelatin immobilization. To assess the capability of the PSi to detect gelatinase enzymes, a solution containing a metalloprotease, MMP-2, was assayed over a range of concentrations. 100 μL of MMP-2 in PBS was added to quartz cuvettes containing the rugate filter. Blue shifts in the reflectivity due to enzyme activity were detected within 3 hours down to 167 pM (fmoles of enzyme, Figure 2). There was no additional blue shift after 3 hours of incubation for all concentration points.

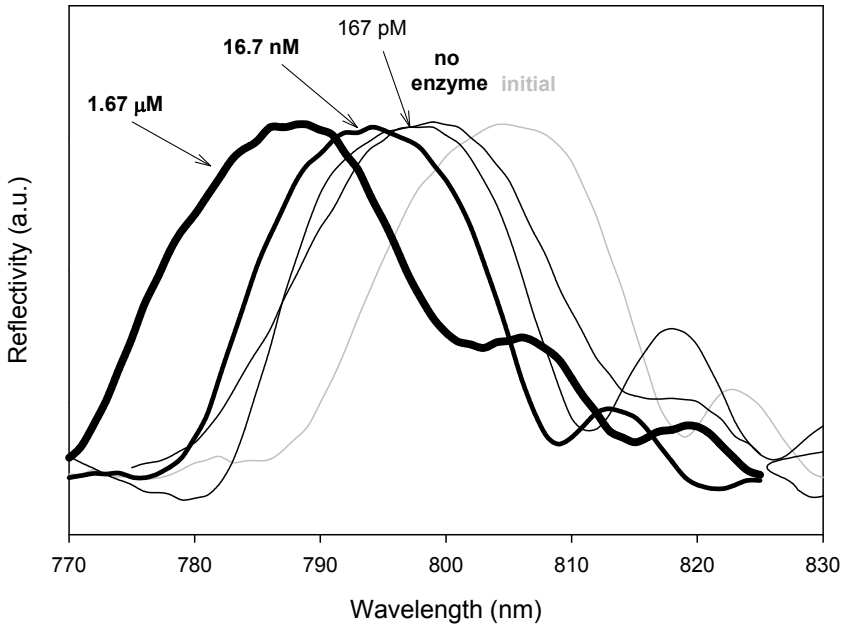

Fig. 2. Reflectivity shift of gelatin loaded rugate filters exposed to different concentrations of MMP-2 after 3 hour incubation at 37° C.

A murine macrophage cell line (J774[16]) was chosen for the present study with lipopolysaccharide (LPS) treatment to stimulate gelatinase secretion.[6, 17-21] LPS treatment of murine macrophages in excess of 10 ng/mL has been shown to cause >10-fold upregulation of MMP-2 and > 50-fold upregulation of MMP-9[18] with a moderate increase in MMP-1 activity (~3-fold)[16]. As an initial test, $1x10^6$ cells in 1 mL of serum were stimulated with 100 ng/mL LPS for 24 hours. After incubation the cells were pelleted by centrifugation, the supernatant removed and applied to gelatin loaded rugate filters for incubation overnight (16 hours) at 37˚ C. Figure 3 shows the change in the high reflectivity peak position after overnight exposure to control (-LPS) and stimulated (+LPS) macrophage supernatants. The optical response to media (±LPS) without cells was used as a further control. The percent of gelatin digested by proteolysis within the rugate filter was 50 – 70 % for the supernatant and attributed to stimulated gelatinase release when normalized to control (Figure 3b).

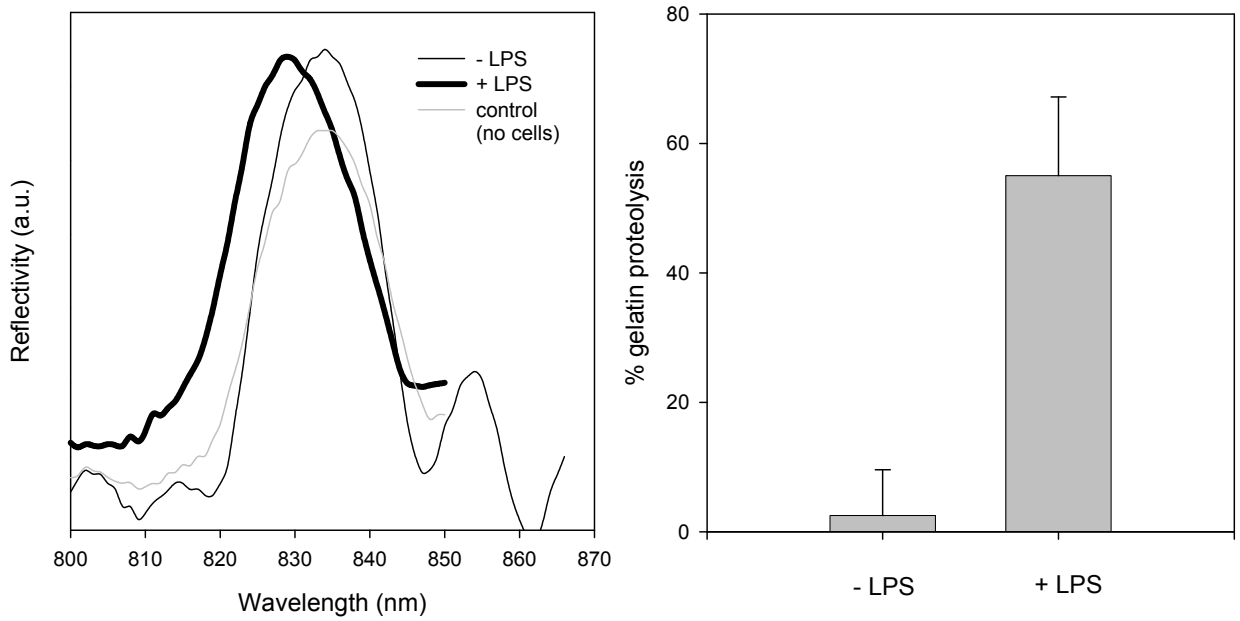

Fig. 3. a) reflectivity shift for macrophage supernatant after 24 hour with and without LPS stimulation including a 'no cell' control (grey), b) average % gelatin proteolysis for three ±LPS experiments using the same supernatant with different PSi samples on different days. % gelatin proteolysis is calculated by dividing the normalized blue shift in the reflectivity by the initial red shift upon gelatin immobilization, all multiplied by 100.

Macrophages are known to adhere to gelatin modified surfaces (standard Petri dish medium) and as such will not require specific capture chemistry. However, after the gelatin has been digested on the surface, the distal chemistry will display antifouling EG molecules which have been shown to discourage cell adhesion.[22] To evaluate if the top surface functionality plays a role with macrophage adhesion, two different surfaces were prepared (Figure 4, left). Firstly, samples were prepared as shown in Figure 1 such that EG_6 molecules would be present at the surface after gelatin digestion (surface 1). For the second sample, the adhesive peptide RGD was first immobilized on the top of the rugate filter followed by interior reaction with EG_6 molecules (surface 2). After the DSC activation step the distal EG moiety (surface 1) and the serine residue of the GRGDS peptide (surface 2) will be activated for coupling primary amines of the gelatin polypeptide.

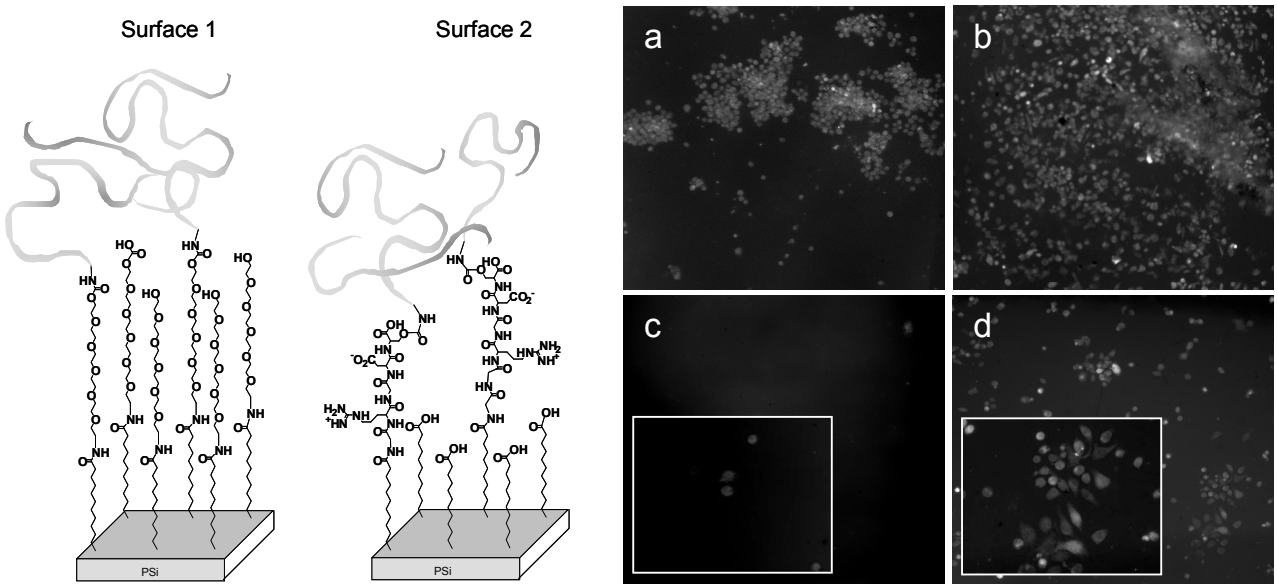

Fig. 4. Different surfaces to be evaluated for macrophage incubation in tissue culture. a) macrophages on the surface of a rugate filter with distal antifouling (surface 1) and b) distal RGD peptides (surface 2). c) and d) rugate filters after PBS rinse.

Figure 4a and b show the surface of the rugate filters after incubation with approximately $5x10^5$ cells (in 500 μL) for 24 hours at 37˚ C. Macrophages stained with CMRA are shown to cluster on the EG_6 terminated sample in small groups across the surface (Figure 4a). In contrast, the RGD terminated surface results in a more even distribution of cells (Figure 4b). In cases where the rugate filters were first rinsed with phosphate buffered saline prior to fixation, the majority of the macrophages on the antifouling surface are removed while considerable cells remain on the RGD-functionalized sample (Figure 4c and d). In addition, macrophages on the RGD terminated filter display an adherent (spreading) morphology suggesting specific binding to RGD and focal adhesion formation.

Distal functionality at the surface leads to different adhesion characteristics of the macrophages. To evaluate the effect that distal chemistry will have on enzyme release, the interfaces depicted in Figure 4 were exposed to stimulated macrophages and the optical reflectivity measured after incubation in tissue culture overnight. Gelatin loaded rugate filters were mounted into individual wells of a 48-well plate with 500 μL of media applied immediately to avoid drying on the interior of the samples. After application of media, the cells were seeded for 1-2 hours to allow adhesion followed by application of 100 ng/mL LPS. Figure 5 shows the reflectivity shifts (top) of the photonic structures after overnight incubation ± LPS for 1) a gelatin loaded rugate filter with RGD peptide on the top of the filter and on the interior (RGD out/RGD in, no internal antifouling character), 2) RGD on the top but with antifouling EG_6 molecules lining the interior of the pore walls (RGD out/EG_6 in, see methods and reference[12] for description of differential chemistry) and 3) antifouling EG_6 on the top and interior of the photonic crystal (EG_6 out/EG_6 in).

From Figure 5, the gelatin loaded rugate filter that does not contain internal antifouling chemistry displays a negative optical response compared to rugate fitlers that contain the antifouling EG_6 molecules internally. LPS stimulation causes release of gelatinases that cleave gelatin leading to a blue shift and positive % gelatin proteolysis as observed with the interfaces containing internal EG_6 moieties. Without antifouling chemistry, the enzymes and biomolecules in the complex media can non-specifically adsorb to the surface thus leading to a red shift and negative % gelatin proteolysis for rugate filters beneath stimulated cells. This demonstrates the importance of antifouling layers at the base of the biorecognition interface in PSi to prevent non-specific protein adsorption in order to accurately detect gelatinolytic activity. After normalization, there was no significant difference between the gelatin filled structures that

contained ± RGD on the top and therefore, the remaining experiments were performed without the use of RGD peptide ligands.

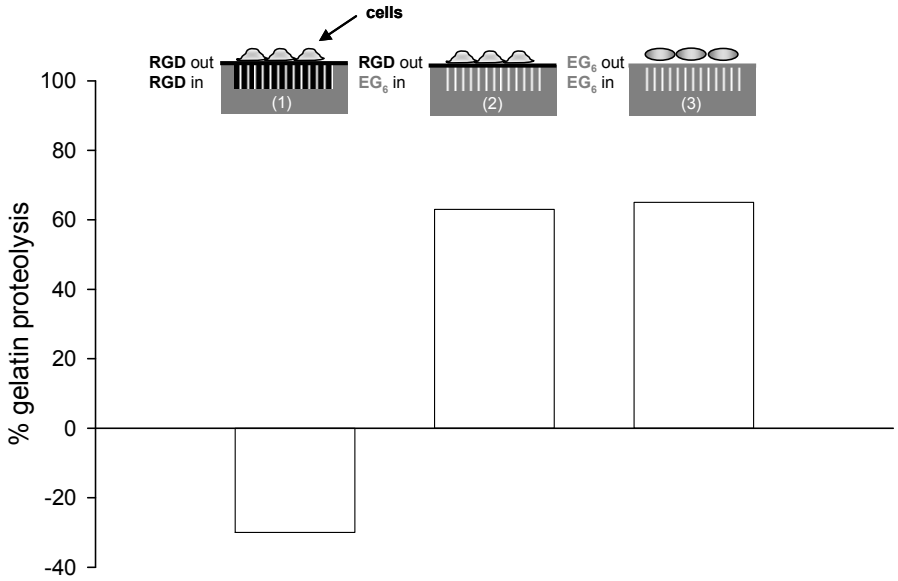

Fig. 5. Comparison of % gelatin proteolysis measured for surfaces presenting different internal and external distal functionality.

To assess the effect of MMP secretion on the same sample over time, optical measurements were taken at time 0, 4 and 22 hours of LPS stimulation (Figure 6a). After 4 hours the reflectivity resonance of the sample exposed to + LPS blue shifted 5 nm (21 % gelatin digested) relative to -LPS. After 22 hours the relative blue shift of the same sample increased to 12 nm (37 % gelatin digested). Similarly, gelatin cleavage by secreted MMPs within rugate filters mounted in culture plates were detected at time points greater than 2 hours with an increase in optical response over time (Figure 6b and c). Figure 6b demonstrates the increasing trend for reflectivity blue shifts within the same run (same cell culture, same day) with three different rugate filters at 6, 8 and 24 hours. The observed blue shift for rugate filters exposed to unstimulated macrophages (- LPS) was approximately the same at different timepoints across samples and thus attributed to some background endogenous gelatinase activity and minor amounts of silicon oxidation. Rugate filters exposed to the same cell populations on a given day tended to cluster in a similar fashion such that differences between macrophage cultures are presumably the major source of variability. Importantly, cells on the surfaces remained viable for the timescales needed for data collection as determined by microscopy. In cases where cell viability was in question[1], the optical response deviated from expectation (Figure 6c, empty square).

Judging from the microscope images, there are approximately 200,000 cells/cm^2 on the surface. With our current optical collection instrument, this corresponds to reflectivity data gathered from the photonic substrate beneath 1,560 cells. In these experiments, there is an optical response to secreted gelatinases after 2 hours with the LPS-induced blue shift increasing with time. Using this approach, endogenous MMP expression is controlled within the same plate using material from the same rugate filter in a separate well. Thus the difference between the optical spectra measured from the photonic crystals can be confidently attributed to stimulated protease enzyme secretion. In contrast to previous work in our group,[23] monitoring proteolysis using adherent cells involves dynamic secretion such that continuous release is measured over time. Incorporating a label-free optical tool into cell culture for non-invasive gelatinolytic activity detection from live cells will have numerous benefits in cell culture including viability assessment, adhesion monitoring and screens for therapeutic development.

[1] Acidification of media upon cell death results in a colour change of the phenol red indicator from a pink colour (neutral physiological pH) to yellow (pH < 7).

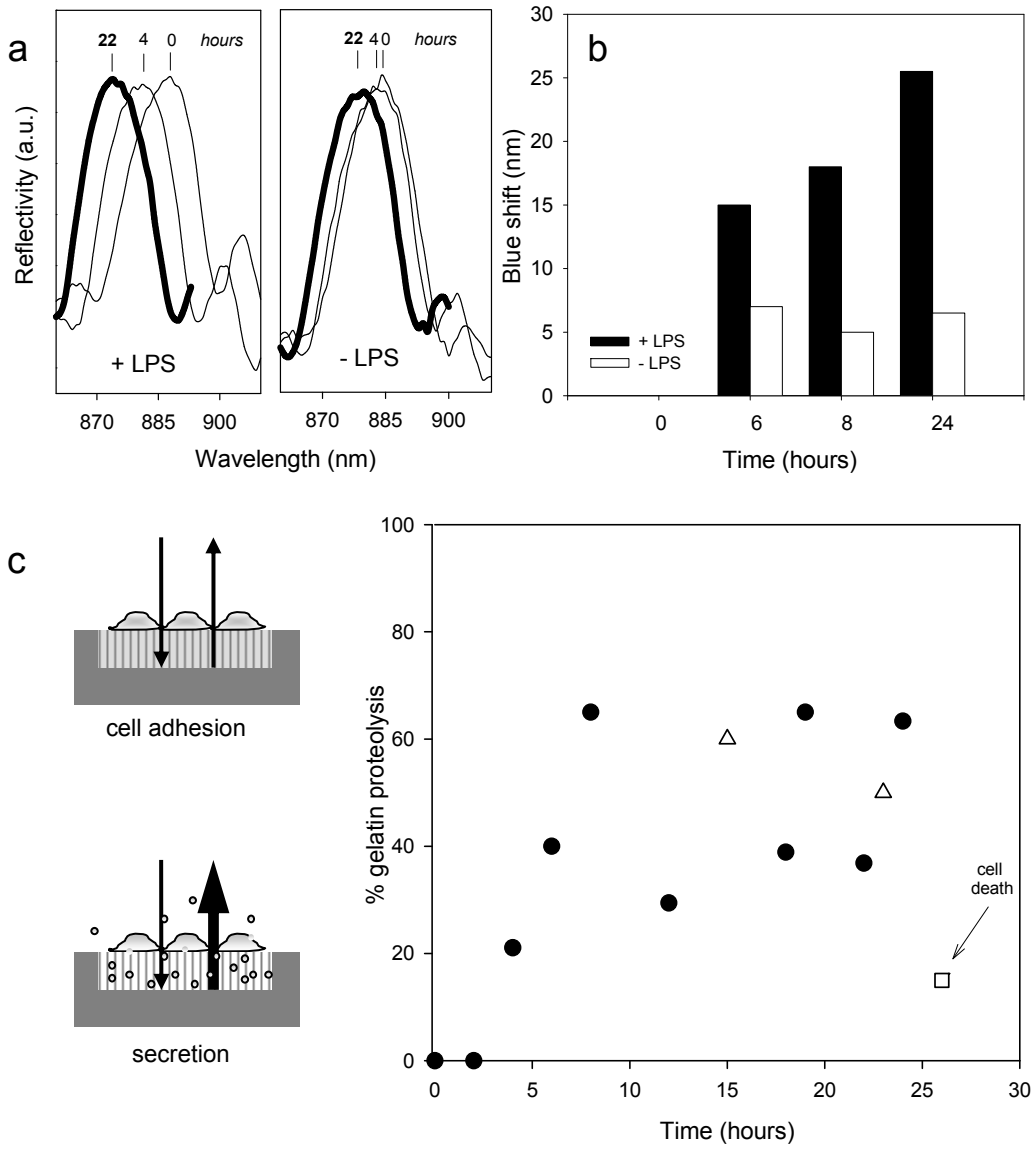

Fig. 6. a) reflectivity shifts of the same rugate filter incubated with J447 macrophages ± LPS measured at t = 0, 4 and 22 hours, b) blue shifts in the reflectivity of three different samples at three different times exposed to the same batch of J447 macrophage culture (± LPS), c) schematic of protease secretion from adherent cells and % gelatin proteolysis for all experiments – triangles represent early experiments with filters exposed to macrophage supernatant (from Figure 2), the square is a rugate filter where the cells died during incubation.

4. CONCLUSIONS

In conclusion, a simple, sensitive and fast optical device based on porous silicon has been demonstrated for monitoring inflammatory responses from cells in tissue culture. Profiling the release of specific MMPs from pathogenic cells, during various treatments and in the presence of inhibitors should find utility for understanding disease progression and developing therapeutics. The sensitive optical response to dynamic protease release from cultured cells will enable the implementation of these complex optical materials into standard cell culture plates for real-time monitoring of cellular secretion and degranulation.

REFERENCES

[1] Kilian, K. A.; Boecking, T.; Gooding, J. J., "The importance of surface chemistry in mesoporous materials: lessons from porous silicon biosensors" Chem. Commun. 6, 630-640, (2009).

[2] Jane, A.; Dronov, R.; Hodges, A.; Voelcker, N. H., "Porous silicon biosensors on the advance" Trends Biotechnol. 27 (4), 230-239 (2009).

[3] Anglin, E. J.; Cheng, L.; Freeman, W. R.; Sailor, M. J., "Porous silicon in drug delivery devices and materials" Adv. Drug Delivery Rev. 60 (11), 1266-1277 (2008).

[4] Stewart, M. P.; Buriak, J. M., "Chemical and Biological Applications of Porous Silicon Technology" Adv. Mater. 12 (12), 859-869 (2000).

[5] Ouyang, H.; Fauchet, P. M., "Biosensing using porous silicon photonic bandgap structures" Proc. SPIE 6005, 1-15 (2005).

[6] Kilian, K. A.; Lai, L. M. H.; Magenau, A.; Cartland, S.; Bocking, T.; Di Girolamo, N.; Gal, M.; Gaus, K.; Gooding, J. J., "Smart Tissue Culture: in Situ Monitoring of the Activity of Protease Enzymes Secreted from Live Cells Using Nanostructured Photonic Crystals" Nano Lett. 9 (5), 2021-2025 (2009).

[7] Bayliss, S. C.; Buckberry, L. D.; Fletcher, I.; Tobin, M. J., "The culture of neurons on silicon" Sens. Actuators, A A74, (1-3), 139-142 (1999).

[8] Bayliss, S. C.; Buckberry, L. D.; Harris, P. J.; Tobin, M., "Nature of the silicon-animal cell interface" J. Porous Mat. 7 (1/2/3), 191-195 (2000).

[9] Ben-Tabou de Leon, S.; Sa'ar, A.; Oren, R.; Spira, M. E.; Yitzchaik, S., "Neurons culturing and biophotonic sensing using porous silicon" Appl. Phys. Lett. 84 (22), 4361-4363 (2004).

[10] Chin, V.; Collins, B. E.; Sailor, M. J.; Bhatia, S. N., "Compatibility of primary hepatocytes with oxidized nanoporous silicon" Adv. Mater. 13 (24), 1877-1880 (2001).

[11] de-Leon, S. B.-T.; Oren, R.; Spira, M. E.; Korbakov, N.; Yitzchaik, S.; Sa'ar, A., "Porous silicon substrates for neurons culturing and bio-photonic sensing" Phys. Stat. Sol. A 202 (8), 1456-1461 (2005).

[12] Kilian, K. A.; Böcking, T.; Gaus, K.; Gooding, J. J., "Introducing distinctly different chemical functionalities onto the internal and external surfaces of mesoporous materials" Angew. Chem., Int. Ed. 47 (14), 2697-2699 (2008).

[13] Sapelkin, A. V.; Bayliss, S. C.; Unal, B.; Charalambou, A., "Interaction of B50 rat hippocampal cells with stain-etched porous silicon" Biomaterials 27 (6), 842-846 (2006).

[14] Schwartz, M. P.; Derfus, A. M.; Alvarez, S. D.; Bhatia, S. N.; Sailor, M. J., "The Smart Petri Dish: A Nanostructured Photonic Crystal for Real-Time Monitoring of Living Cells" Langmuir 22 (16), 7084-7090 (2006).

[15] Ilyas, S.; Boecking, T.; Kilian, K.; Reece, P. J.; Gooding, J.; Gaus, K.; Gal, M., "Porous silicon based narrow line-width rugate filters" Opt. Mater. 29 (6), 619-622 (2007).

[16] Hong, C.-Y.; Lin, S.-K.; Kok, S.-H.; Cheng, S.-J.; Lee, M.-S.; Wang, T.-M.; Chen, C.-S.; Lin, L.-D.; Wang, J.-S., "The role of lipopolysaccharide in infectious bone resorption of periapical lesion" J. Oral Pathol. Med. 33 (3), 162-169 (2004).

[17] Speidl, W. S.; Toller, W. G.; Kaun, C.; Weiss, T. W.; Pfaffenberger, S.; Kastl, S. P.; Furnkranz, A.; Maurer, G.; Huber, K.; Metzler, H.; Wojta, J., "Catecholamines potentiate LPS-induced expression of MMP-1 and MMP-9 in human monocytes and in the human monocytic cell line U937: possible implications for peri-operative plaque instability" FASEB J. 18 (3), 603-605 (2004).

[18] Xie, B.; Dong, Z.; Fidler, I. J., "Regulatory mechanisms for the expression of type IV collagenases/gelatinases in murine macrophages" J. Immunol. 152 (7), 3637-44 (1994).

[19] Rhee, J. W.; Lee, K.-W.; Kim, D.; Lee, Y.; Jeon, O.-H.; Kwon, H.-J.; Kim, D.-S., "NF-kB-dependent regulation of matrix metalloproteinase-9 gene expression by lipopolysaccharide in a macrophage cell line RAW 264.7" J. Biochem. Molec. Biol. 40 (1), 88-94 (2007).

[20] Woo, C.-H.; Lim, J.-H.; Kim, J.-H., "Lipopolysaccharide induces matrix metalloproteinase-9 expression via a mitochondrial reactive oxygen species-p38 kinase-activator protein-1 pathway in Raw 264.7 cells" J. Immunol. 173 (11), 6973-80 (2004).

[21] Ogawa, K.; Funaba, M.; Mathews, L. S.; Mizutani, T., "Activin A stimulates type IV collagenase (matrix metalloproteinase-2) production in mouse peritoneal macrophages" J. Immunol. 165 (6), 2997-3003 (2000).

[22] Mrksich, M., "Using self-assembled monolayers to model the extracellular matrix" Acta Biomater. 5 (3), 832-841 (2009).

[23] Kilian, K. A.; Böcking, T.; Gaus, K.; Gooding, J. J., "Peptide-Modified Optical Filters for Detecting Protease Activity" ACS Nano 1 (4), 355-361 (2007).